Compressor cascade correlations modelling at design points using artificial neural networks

P. Kovář ^{a,b,*}, J. Fürst ^{a}

^{a} *Department of Technical Mathematics, Faculty of Mechanical Engineering, Czech Technical University in Prague, Karlovo náměstí 13, 121 35 Praha, Czech Republic*
^{b} *Center of Avionics and Space Research, Faculty of Mechanical Engineering, Czech Technical University in Prague, Jugoslávských partyzánů 1580/3, 160 00 Praha, Czech Republic*

Abstract

In recent years, the flow analysis by means of computational fluid dynamics (CFD) has become a useful design and optimization tool. Unfortunately, despite advances in the computational power, numerical simulations are still very time consuming. Thus, empirical correlation models keep their importance as a tool for early stages of axial compressor design and for prediction of basic performance parameters. These correlations were developed based on experimental data obtained from 2D measurements performed on cases of classical airfoils such as the NACA 65-series or C.4 profiles. There is insufficient amount of experimental data for other families of airfoils, but CFD simulations can be used instead and their results correlated using artificial neural networks (ANN), as described in this work. Unlike the classical deep learning approach using perceptrons, this work presents neural networks employing higher order neural units.
© 2023 University of West Bohemia.

1. Introduction

When subsonic flows corresponding to low Mach number occur, well-known profiles such as the NACA 65-series and C.4 circular-arc are suitable. In cases when the flow is accelerated to high subsonic, transonic or even to low supersonic velocities, double-circular arc and multi-circular arc profiles are able to operate with high efficiency [1]. A special family of airfoils are so-called controlled diffusion (CD) airfoils, which are used for subsonic and transonic applications and they can provide better performance than the aforementioned airfoils. A construction of the shape uses a concept of shaping the blade beyond the point of peak suction of the surface velocity such that the diffusion rate and associated suction boundary layer result in minimum loss for the airfoil [14] resulting in tight range of acceptable incidence angles [1].

Achieving stable design conditions can be very tricky in real operation, especially in real engineering applications, e.g., cooling of a nuclear reactor using an axial compressor placed in the secondary system. Thus, it is necessary to ensure reliable running of the device when off-design conditions occur, e.g., when the incidence angle differs from the design one or parameters of the medium change. The new family of the airfoils introduced in [9] should outperform the classical NACA 65-series, the performance should be comparable with the CD airfoils and the span of incidence angles, until stall occurs, should be much wider. The camber line of the profile and its thickness distribution are defined according to the desired pressure distribution on the blade surface.

---

*Corresponding author. E-mail: patrik.kovar@fs.cvut.cz.

Flow analysis by means of computational fluid dynamics (CFD) can be still very time consuming, thus, empirical correlations are commonly used as a tool for design and prediction of axial compressor cascade performance. Unfortunately, there is not sufficient amount of experimental data in case of other families of airfoils except the classical profiles, and thus, there are no correlations for them. The present work deals with searching similar relations that will serve for other family of airfoils in the same manner as correlations from the literature. The current paper is an extension of the total pressure loss correlation model for design points of an axial compressor cascade designed with a new family of airfoils presented in [10]. Furthermore, design flow parameters, such as the angle of attack α^*, the incidence angle i^*, and the deviation angle δ^*, are modelled using an artificial neural network (ANN) to accelerate the design of a compressor cascade.

Basic concepts of empirical models in an axial compressor cascade are discussed. Basics of higher order neural networks (HONNs) together with supervised learning methods are presented. Empirical correlations from the literature are compared to a function learned by ANN. It turns out that the approach using ANN fits the data obtained by means of CFD much better than the correlations from the literature for cases of profiles studied in the presented work. The workflow of the methodology to predict flow parameters is introduced. Finally, one geometrical setup of the cascade is selected, which was not included in the training data set, and the prediction of flow parameters is tested. Results obtained by ANNs outperformed available correlations from the literature for the studied family of airfoils and proved their ability to be a useful tool during the initial stages of axial compressor design.

2. Objective statement

Firstly, let us introduce geometrical parameters in the compressor cascade. As can be seen in Fig. 1 (top), parameter c stands for the blade chord, parameters a, b denote the point where the maximum of the camber line is reached and symbols χ_1, χ_2 represent blade angles relative to the chord line. Subscripts 1 and 2 are used to distinguish conditions at the inlet and the discharge of the blade, respectively. Angle θ is the sum of blade angles, $\theta = \chi_1 + \chi_2$.

In the case of a cascade, Fig. 1 (bottom), there is a stagger or setting angle γ, which is the angle between the chord line and the axial direction, and blade angles κ_1, κ_2 between the camber line and the axial direction at the leading and trailing edges. The density of the blades is expressed by the solidity $\sigma = c/s$. The flow is described by the velocities W_1, W_2 and the flow angles with the axial direction β_1, β_2. Further, there are the incidence angle i, the deviation angle δ and the angle of attack α defined in [1] as

$$\alpha = \beta_1 - \gamma, \quad \kappa_1 = \chi_1 + \gamma, \quad \kappa_2 = \gamma - \chi_2, \quad i = \beta_1 - \kappa_1, \quad \delta = \beta_2 - \kappa_2. \tag{1}$$

2.1. About difficulties related to design point finding by CFD

In recent years, the flow analysis by computational fluid dynamics has become a useful design and optimization method. Despite advances in computational power, it can still be very demanding to perform a series of numerical simulations. To obtain conditions at the design point, it is necessary to find the correct value of the design angle of attack α^* or the incidence angle i^*, as can be seen in Fig. 2.

In Fig. 2 (bottom), the procedure how a design point can be found is indicated. Through a series of simulations with different boundary conditions and loss evaluations, the point with the smallest pressure loss (*PL*) is said to be the design point.
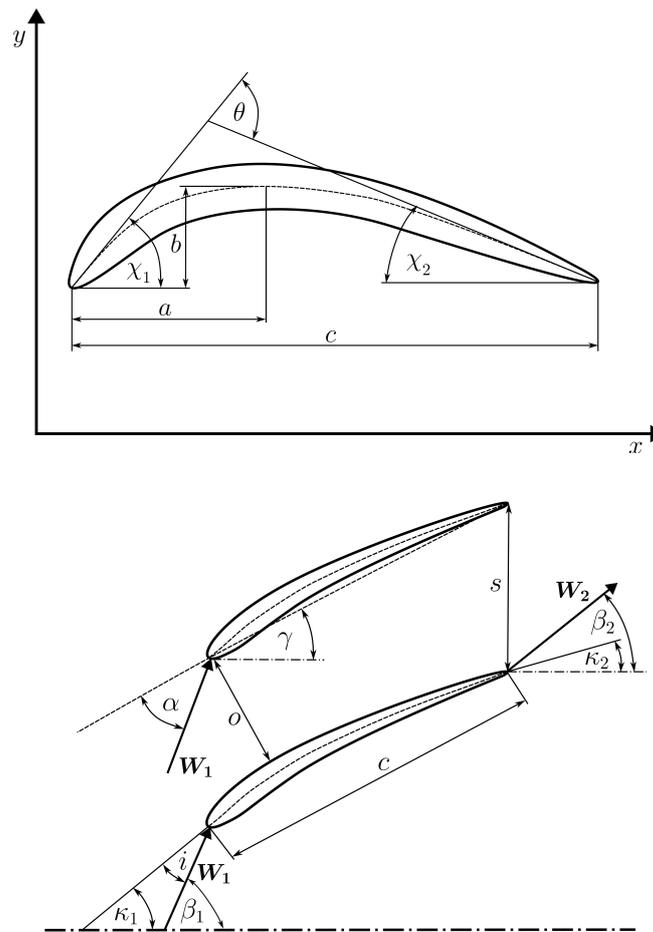
Fig. 1. Cascade nomenclature: (*top*) profile parameters, (*bottom*) cascade and flow parameters

2.2. About empirical correlations

The basic objective of the empirical modelling process is to predict the fluid turning and the total pressure loss for a cascade under fairly general operating conditions [1]. The empirical correlations are derived from experimental data obtained from two-dimensional (2D) measurements.

2.2.1. Design angle of attack α^* and incidence angle i^*

The design angle of attack α^*, or the design incidence angle i^*, define a near-optimum or minimum-loss inlet angle for the cascade. The selection of α^* was based on achieving smooth blade surface pressure distributions, particularly on the suction surface. In [6], Herrig et al. formulated the following empirical model:

$$\alpha^* = \left[3.6 K_{sh} K_{t,i} + 0.3532\, \theta \left(\frac{a}{c}\right)^{0.25}\right] \sigma^e, \quad e = 0.65 - 0.002\, \theta, \tag{2}$$

where the correction factor K_{sh} is assumed to be constant for a specific family of airfoils and the parameter $K_{t,i}$ can be correlated as a function of the maximal blade thickness-to-chord ratio t_b/c [1]

$$K_{t,i} = \left(10\, \frac{t_b}{c}\right)^q, \quad q = \frac{0.28}{0.1 + \left(\frac{t_b}{c}\right)^{0.3}}. \tag{3}$$
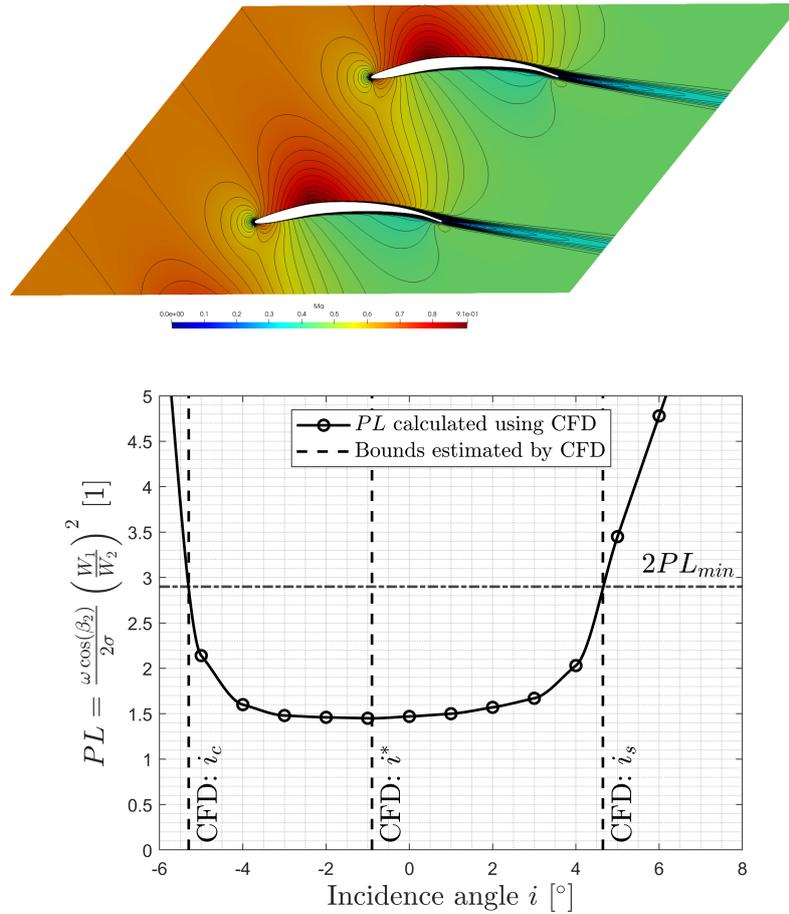
Fig. 2. CFD post processing: (*top*) flow field example, (*bottom*) design point finding

Since the parameter K_{sh} and the ratios t_b/c, a/c are constant, the parameter $K_{t,i}$ is also constant for the studied family of airfoils and the issue can be simplified to a function of two variables $\alpha^* = f(\sigma, \theta)$.

The design incidence angle i^* correlation was developed by Lieblein in [11]

$$i^* = K_{sh}K_{t,i}(i^*)_{(10)} + n\theta. \tag{4}$$

The first term on the right-hand side is the design incidence angle for a camber angle of zero. It is computed from a correlation for NACA 65-series blades and corrected by K_{sh} and $K_{t,i}$

$$(i_0^*)_{(10)} = \frac{\beta_1^p}{5 + 46\exp(-2.3\sigma)} - 0.1\sigma^3\exp\left(\frac{\beta_1 - 70}{4}\right), \quad p = 0.914 + \frac{\sigma^3}{160}. \tag{5}$$

According to [8], the slope factor n can be expressed as

$$n = 0.025\,\sigma - 0.06 - \frac{\left(\frac{\beta_1}{90}\right)^{(1+1.2\sigma)}}{1.5 + 0.43\sigma}. \tag{6}$$

Unlike the correlation for α^* except for σ and θ, the flow angle at the cascade inlet β_1 appears in the equations, thus, the design incidence angle i^* should be modelled as $i^* = f(\sigma, \theta, \beta_1)$.

2.3. Design deviation angle δ^*

There is also an empirical model for the design deviation angle δ^* supplied by Lieblein in [12] that corresponds to operation at the design incidence angle i^*. The model has similar form as the design incidence angle correlation discussed above

$$\delta^* = K_{sh}K_{t,\delta}(\delta_0^*)_{(10)} + m\theta. \tag{7}$$

The coefficient K_{sh} is the same as for the design incidence angle model and the parameter $K_{t,\delta}$ is correlated as

$$K_{t,\delta} = 6.25\left(\frac{t_b}{c}\right) + 37.5\left(\frac{t_b}{c}\right)^2. \tag{8}$$

The design zero-camber deviation angle $(\delta_0^*)_{(10)}$ from [8] can be obtained as

$$(\delta_0^*)_{(10)} = 0.01\sigma\beta_1 + (0.74\sigma^{1.9} + 3\sigma)\left(\frac{\beta_1}{90}\right)^{(1.67+1.09\sigma)}. \tag{9}$$

Defining $x = 0.01\beta_1$, the slope factor m for the NACA 65-series camberline is modelled as [1]

$$m = \frac{m_{1.0}}{\sigma^b}, \quad m_{1.0} = 0.17 - 0.0333\,x + 0.333x^2, \quad b = 0.9625 - 0.17x - 0.85x^3. \tag{10}$$

One can see that the issue is the same as in the case of the previous incidence angle correlation, the design deviation angle can be modelled as $\delta^* = f(\sigma, \theta, \beta_1)$.

2.4. Total pressure loss PL

In [12], Lieblein developed an empirical correlation for pressure loss PL as a function of the equivalent diffusion factor D_{eq} [13], based on experimental cascade data for the NACA 65-series and C.4 circular-arc blades as

$$PL = \frac{\omega\cos\beta_2}{2\sigma}\left(\frac{W_1}{W_2}\right)^2 = K_1\left[K_2 + 3.1\left(D_{eq} - 1\right)^2 + 0.4\left(D_{eq} - 1\right)^8\right], \tag{11}$$

where $K_1 = 0.004$, $K_2 = 1$ and

$$D_{eq} = \left(\frac{W_{max}}{W_1}\right)\frac{W_1}{W_2} = \left[1.12 + 0.61\frac{\cos^2\beta_1}{\sigma}\left(\tan\beta_1 - \tan\beta_2\right)\right]\frac{W_1}{W_2}. \tag{12}$$

In the present paper, the pressure loss is modelled as $PL = f(D_{eq})$. As can be seen in the equations above, the dependency between the monitored parameters (α^*, i^*, δ^*, PL), the cascade parameters and the parameters of the flow is strongly non-linear, making it a suitable task for ANN.

3. Methodology

Basic ideas on the working of higher order neural networks, the learning process and approximate error evaluation are introduced in this section. Finally, the procedure of flow parameters prediction is presented together with a clear flowchart.
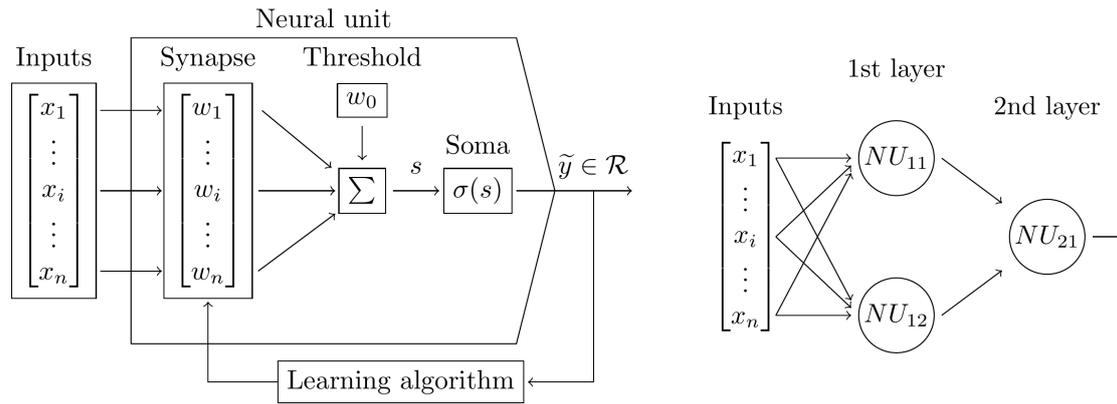
Fig. 3. Neural network: (*left*) single neural unit, (*right*) shallow neural network

3.1. Basic ideas of higher order neural networks

The information processing within a neural unit consists of two separated mathematical operations [4]. The first of them is a so-called synaptic operation, which receives inputs and combines them with neural weights that represent some kind of memory. A somatic operation can be responsible for introducing nonlinearities such as thresholding, non-linear activation, aggregation, etc. A neural output $\widetilde{y}$ of the individual unit is a scalar as can be seen from

$$\widetilde{y} = \sigma(s) \tag{13}$$

and continues as a nerve impulse into the next layer of neural units as indicated in Fig. 3 (left).

The N-th order synaptic operation of the neural unit can be written as [5]

$$s = w_0 x_0 + \sum_{i=1}^{n} w_i x_i + \sum_{i=1}^{n} \sum_{j=i}^{n} w_{ij} x_i x_j + \cdots + \sum_{i_1=1}^{n} \cdots \sum_{i_N=i_{N-1}}^{n} w_{i_1 i_2 \ldots i_n} x_{i_1} x_{i_2} \ldots x_{i_n}, \tag{14}$$

where $x_0 = 1$ stands for the threshold and n denotes the length of the input feature vector.

Since samples in the training data set are labelled, neural network does supervised learning, which is the task of learning a function that maps inputs to desired outputs. The weight of similarity between the neural outputs and the true outputs is represented with the cost function

$$\vec{e} = \overrightarrow{\widetilde{Y}} - \vec{Y}. \tag{15}$$

It is evident that the error is strongly dependent on neural memories represented by the vector of weights $\vec{W}$. Thus, the processing of information should be done in a way that leads to the neural unit being learned. For this purpose, the gradient descent batch Levenberg-Marquardt algorithm for weights updating [4] is employed in this work

$$\vec{W} = \vec{W} + \Delta\vec{W}, \tag{16}$$

$$\Delta\vec{W}^T = -\left(\vec{\vec{J}}^T\vec{\vec{J}} + \frac{1}{\mu}\vec{\vec{I}}\right)^{-1}\vec{\vec{J}}^T\vec{e}. \tag{17}$$

The coefficient μ is the learning rate, $\vec{\vec{I}}$ is the $n_w \times n_w$ identity matrix, n_w is the number of weights, and $\vec{\vec{J}}$ represents the $n \times n_w$ Jacobian matrix.
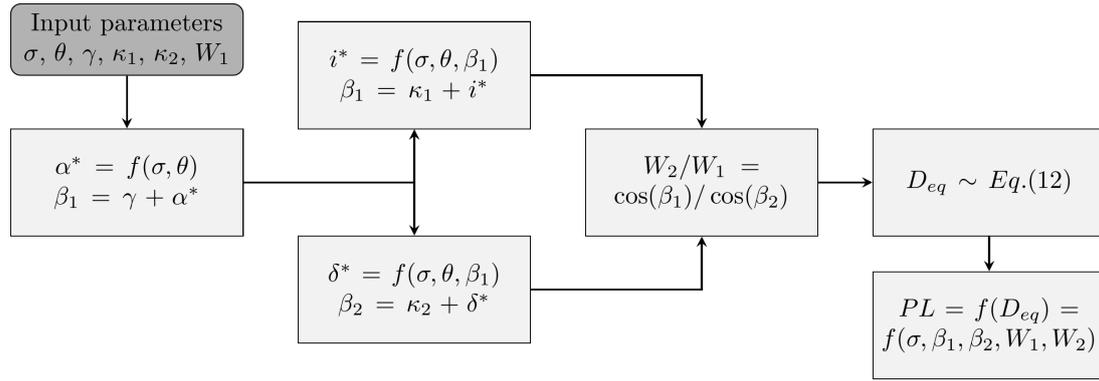
Fig. 4. Workflow for flow parameters prediction

It is convenient to divide the training data set, which in this case contains 48 samples, into three parts. The first one, usually the largest part, serves for learning and weights updating. The validating set serves for error estimation after each learning epoch, which gives us a check if neural network is not overtrained. The learning algorithm continues until this error starts increasing. The last part measures the error after learning termination. The testing error is measured as a mean squared error (MSE) defined as

$$\text{MSE} = \frac{1}{n} \sum_{i=1}^{n} \left(y_i - \widetilde{y}_i \right)^2 . \tag{18}$$

The composed shallow neural network is assembled with two neurons in the first layer and a single neuron in the output layer, as indicated in Fig. 3 (right). A quadratic polynomial synaptic operation was prescribed to the whole network. A bipolar sigmoid activation function $\sigma(\cdot)$ was selected for the first layer. Linear activation was employed in the output layer. The multilayer backpropagation algorithm, described in [5], was used for the error propagation in this work.

3.2. Getting all working together to predict flow parameters

The procedure starts with the calculation of α^*. Because there are only two parameters necessary as inputs, it can give an estimation based on purely geometrical parameters of the cascade, i.e., σ, θ. Then, one can make an estimation of the flow angle β_1 as described in (1) and compute the angles i^* and δ^* using trained neural networks. Since the flow angles β_1 and β_2 are calculated, the only unknown parameter is the velocity at the cascade outlet W_2. The ratio W_2/W_1 can be determined by the following relation [3]:

$$W_1 \cos \beta_1 = W_2 \cos \beta_2. \tag{19}$$

Now all parameters necessary to calculate the equivalent diffusion ratio D_{eq} described by (12) are known and the last correlation for the design total pressure loss PL can be applied as indicated by the prediction workflow in Fig. 4.

4. Results

To obtain a data set without experimental measurements, CFD simulations seem to be a sufficient compromise. Thus, simulations under different geometrical setups and inlet boundary

conditions were done, e.g., in [2]. According to [1], the design point of the cascade can be found as the flow under the incidence angle with the lowest pressure loss.

The obtained data are subjected to several investigations. Firstly, to standard method – optimization of the coefficient in generalized empirical relations for monitored quantities by means of least squares. Secondly, an approach using neural networks is applied and the obtained results are compared with the calculated data. Finally, a comparison on the airfoil that was excluded from the data set to prove the applicability of the proposed correlations is performed.

4.1. An approach using the least squares method

Since the empirical correlations can be generalized using the coefficients as K_{SH}, K_1, K_2 and the functions for $m_{1.0}$ and b, the initial attempt should be to find these parameters for a new family of airfoils. It could be done by using the least squares method to fit the data obtained through CFD.

In the case of the total pressure loss PL correlation, there are two coefficients K_1, K_2 to be found. The optimization was performed using the standard Nelder-Mead algorithm implemented in the MATLAB framework. Equation (18) was chosen as the cost function to measure the error. It turned out that the coefficient K_1 should be equal to 0.0035 and K_2 should stay equal to one.

Another case is the optimization of the K_{SH} coefficient that appears in several correlations. At first sight, the coefficient should be the same for all the correlations where it plays its role. Fitting of the parameters was done, when the cost function was assumed as a sum of MSE performed on the data for both the design angle of attack α^* and the incidence angle i^*. It turned out that the coefficient performs better than the correlations from the literature only in the case of α^*, as can be seen in Table 1 and the following Tables 3 and 4. Hence, the coefficient K_{SH} was later assumed to be independent of the quantity and fitted for individual correlation separately.

Table 1. The resulting values of K_{SH} and comparison of performed MSE

Interval	K_{SH}	MSE : α^*	MSE : i^*
Optimized to MSE$_{\alpha^*+i^*}$	0.929	6.760	4.434
Optimized to MSE$_{\alpha^*}$	0.351	4.511	8.952
Optimized to MSE$_{i^*}$	1.164	14.481	3.523

Based on the knowledge from previous coefficients optimization, it turned out that in order to reach the best match with the CFD data, the coefficient K_{SH} should be fitted individually for each of the searched correlations.

Unlike the previous scalar coefficients K_{SH}, K_1, K_2, the parameters m and b are functions of the variable x, thus, the finding of these unknowns is performed as an optimization of polynomials $\mathcal{P}$

$$\mathcal{P}_{m_{1.0},b} = a_{0,m_{1.0},b} + a_{1,m_{1.0},b}x + a_{2,m_{1.0},b}x^2 + a_{3,m_{1.0},b}x^3. \tag{20}$$

To sum it up, finding the best match with CFD data in the sense of the least squares method leads to the optimization of nine parameters. The K_{SH} value for the design incidence angle δ^* was found as $K_{SH} = 1.951$. Finally, plots of the functions found as the best fitting for the design deviation angle δ^* together with $m_{1.0}$ for the NACA-65 and circular arc profiles can be seen in
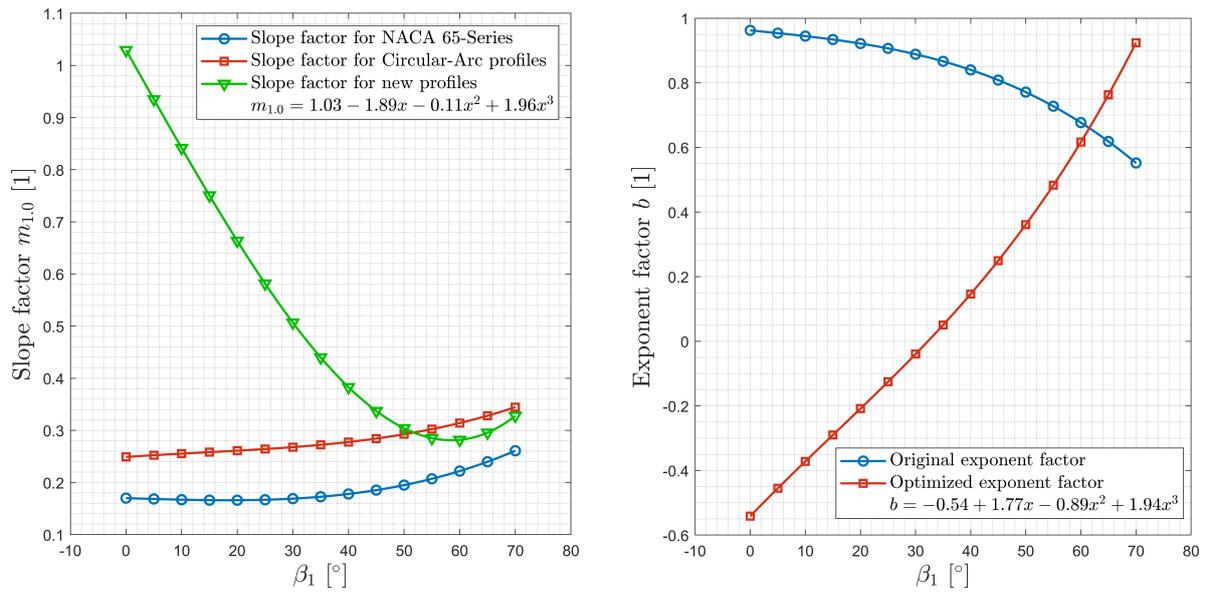
Fig. 5. Optimized functions: (*left*) slope factor $m_{1.0}$, (*right*) exponent factor b

Fig. 5 (left). The trend of found b function against the original function from the literature can be seen in Fig. 5 (right).

4.2. An approach using neural networks

The data set was split into three parts, 80 % of the samples belong to the training subset and the rest was equally distributed to the validating and testing subsets. The learning rate in the weights updating formula (16) was set to $\mu = 0.4$.

4.2.1. Correlation for the design total pressure loss (PL)

Twenty epochs were enough for the neural network to learn with a testing error of 0.016 3, as it is shown in Fig. 6 (left). Fig. 6 (right) shows a comparison of the function learned by ANN and the Lieblein's correlation with the whole data set obtained using CFD.

Table 2 lists deviations measured using MSE. The results obtained by the Lieblein's correlation, the generalized correlation with optimized coefficients K_1, K_2, and by the ANN approach are related to data obtained by CFD. As can be seen, an approximation by ANN is more than three times more accurate than the Lieblein's correlation model and almost three times more precise than the optimized version of the correlation in the whole interval of the equivalent diffusion ratio D_{eq}. In the region of interest, i.e., under the diffusion limit ($D_{eq} < 2$) that refers to a limit, beyond which an abrupt increase in the pressure loss can be expected, the difference between the discussed methods is smaller but the ANN method is still almost twice more accurate compared to the Lieblein's correlation. The relation with optimized coefficients $K_1 = 0.003\,5$, $K_2 = 1$ showed even a higher error in the region $D_{eq} < 2$ that corresponds to a three times higher difference than the approach using ANN.

4.3. Correlation for design angle of attack (α^*)

Graphical comparisons of the correlations from the literature and the neural network approach are shown in Fig. 7. The design angle of attack α^* is a function of two variables, unlike the design total pressure loss correlation. To clarify the meaning of the following comparisons, i.e.,

Table 2. MSE comparison for design total pressure loss PL

Correlation	Literature	Optimized	ANN	Lit./ANN	Opt./ANN
MSE : $D_{eq} < 2$	0.157	0.244	0.090	1.744	2.711
MSE : whole interval	0.356	0.303	0.109	3.244	2.779

the design incidence angle i^* and the design deviation angle δ^*, there are two figures for the α^* correlation. In Fig. 7 (left), there is a comparison in the $\{\sigma, \theta\}$ space. The same results are shown in Fig. 7 (right) but in dependence on the serial number of sample.

The results displayed in Fig. 7 (right) give a better idea of the error size. This is especially true if the function depends on more than two variables, as will be shown below.

The ability to predict the design angle of attack by ANN and by the correlation from the literature is listed in Table 3. The accuracy of the neural network approach in terms of MSE outperformed the original correlation developed by Herrig et al. more than eight fold. In the case of the optimized coefficient $K_{SH} = 0.351$, there is an improvement of the approximation quality, but the error is still more than five times higher in comparison with ANN.

Table 3. MSE comparison for design angle of attack α^*

Correlation	Literature	Optimized	ANN	Lit./ANN	Opt./ANN
MSE : α^*	7.343	4.511	0.886	8.288	5.091

4.4. Correlations for the design incidence and deviation angles (i^*, δ^*)

The correlations for the design incidence angle i^* and the design deviation angle δ^* were modelled using the same neural network architecture as for the previous correlations. In the case of the design incidence angle i^*, the coefficient K_{SH} was set to 0.351 and $K_{SH} = 1.951$ was
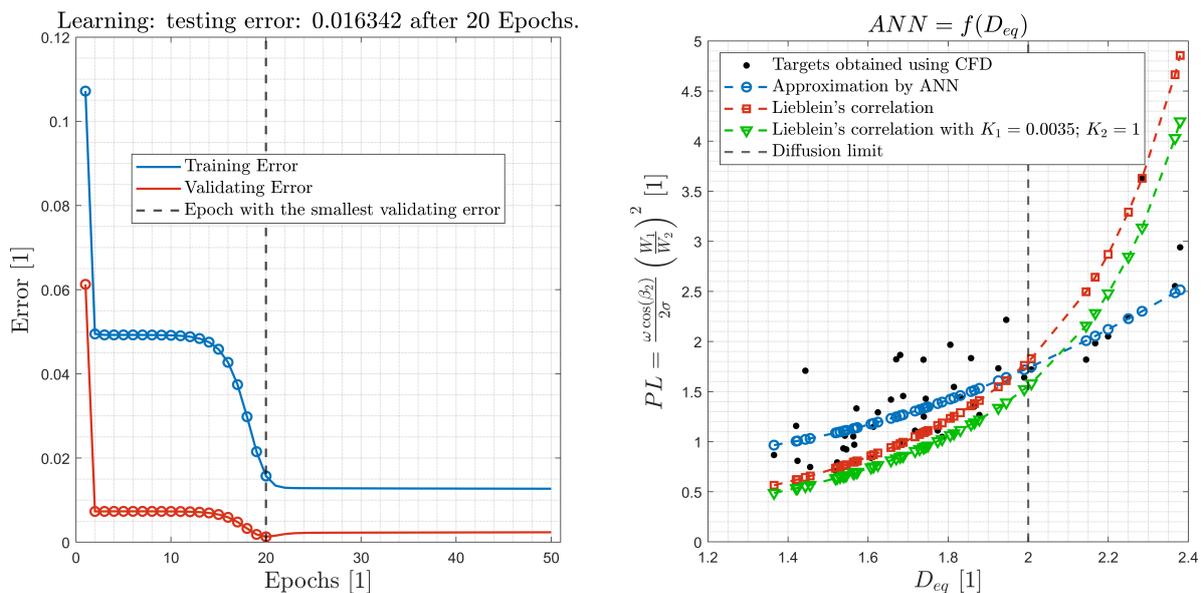
Fig. 6. Progress of learning (*left*), ANN results compared to the Lieblein's correlation (*right*)
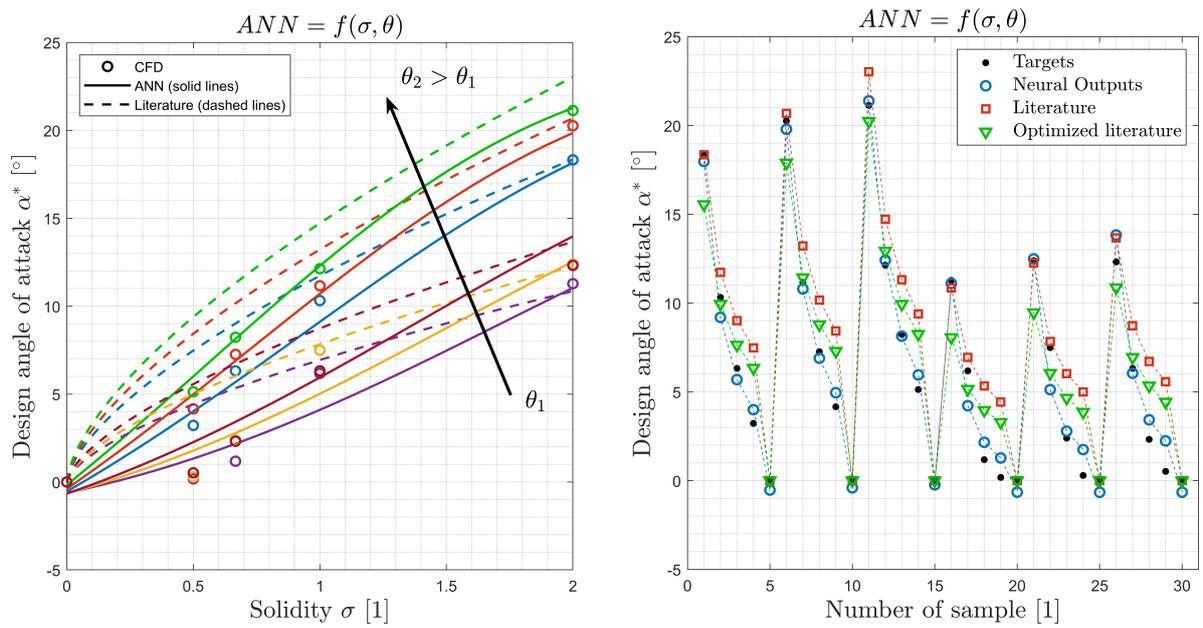
Fig. 7. Results: (*left*) design angle of attack α^* correlation comparison in the $\{\sigma, \theta\}$ space, (*right*) design angle of attack α^* correlation comparison against the number of samples
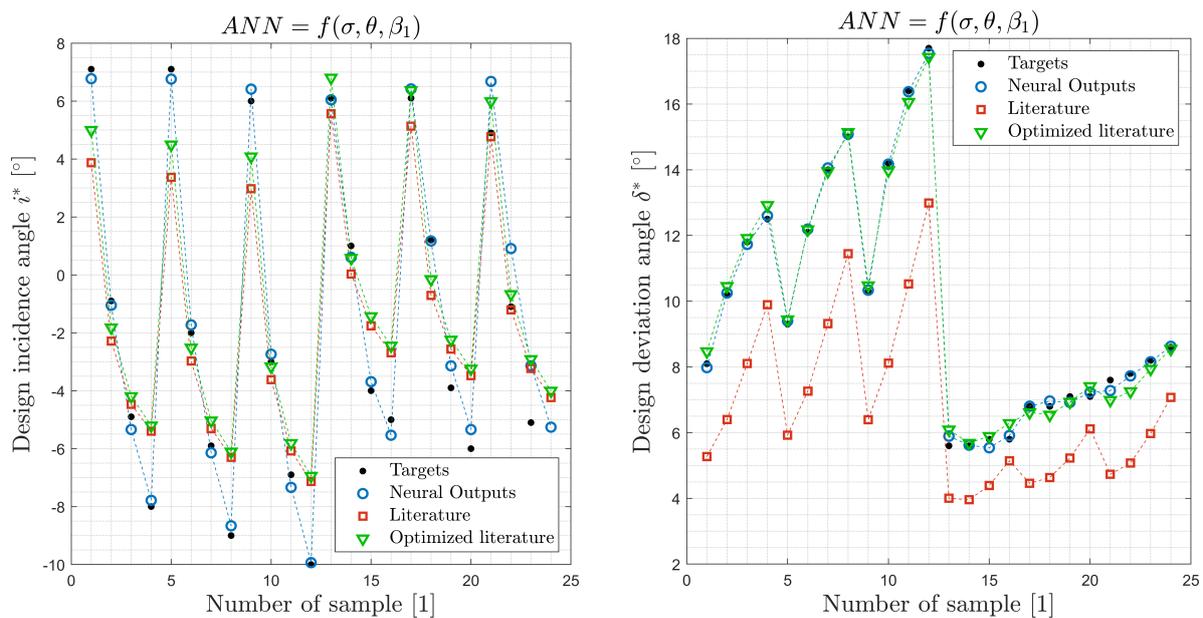
Fig. 8. Results: (*left*) design incidence angle i^* correlation comparison, (*right*) design deviation angle δ^* correlation comparison

set for the design deviation angle δ^*. The coefficients in the formulas for the slope factor $m_{1.0}$ and for the exponent factor b are selected, as is presented in Fig. 5. Since these relations are assumed to be functions of three variables, they are shown only as a comparison against the serial number of sample, as can be seen in Fig. 8.

A performance comparison is listed in Table 4. At first sight, it can be seen that the original correlations from the literature lack the ability to predict both the design incidence and the deviation angles. In the case of the design incidence angle i^*, ANN showed seventeen fold higher

accuracy in comparison with the original literature correlation. When the coefficient K_{SH} is optimized, the error is lower but still of the same order of magnitude. Another case is the investigation of correlation for the design deviation angle δ^* when nine parameters were optimized, as discussed in the previous section. Except for the K_{SH} coefficient, eight parameters in polynomial functions representing factors $m_{1.0}$ and b were also optimized in this case. Although MSE is five times higher than the one from the ANN approach, it is two orders of magnitude more precise than the original literature correlation developed by Lieblein.

Table 4. MSE comparison for design incidence angle i^* and deviation angle δ^*

Correlation	Literature	Optimized	ANN	Lit./ANN	Opt./ANN
MSE : i^*	3.967	3.523	0.233	17.026	15.120
MSE : δ^*	4.640	0.091	0.018	257.778	5.056

4.5. Flow parameters prediction for an airfoil excluded from the training data set

Finally, there is a test of neural network predictions performed on a cascade geometry, which was not included in the training data set, specifically a cascade with solidity $\sigma = 1.25$, blade angle between the camberline and the axial direction at the leading edge $\kappa_1 = 40°$ and $\theta = 30°$.

Referring to the flowchart in Fig. 4, the angle of attack can be calculated based on known cascade parameters. Since the inlet flow angle β_1 can be estimated, it is possible to determine the angles i^* and δ^* using trained neural networks. Thus, the flow angles β_1 and β_2 can be calculated, as well. The only unknown parameter is the velocity at the cascade outlet W_2, which can be calculated using (19). Since all parameters to calculate the equivalent diffusion ratio D_{eq} described by (12) are known, the correlation for the design total pressure loss PL can be applied.

The results of the described procedure are shown in Fig. 9. In this studied case, only the design angle of attack α^* was predicted more accurately by both literature correlations – the original and the one with optimized coefficients – than the approach by ANN. It turned out that
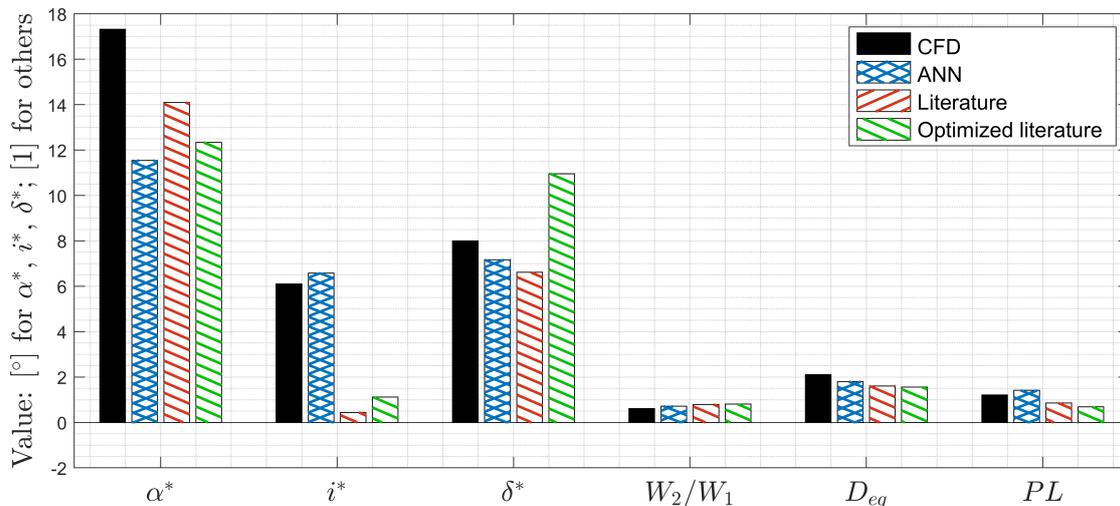
Fig. 9. Comparison of flow field parameters obtained by CFD, ANN and literature correlations performed on the profile excluded from the training data set
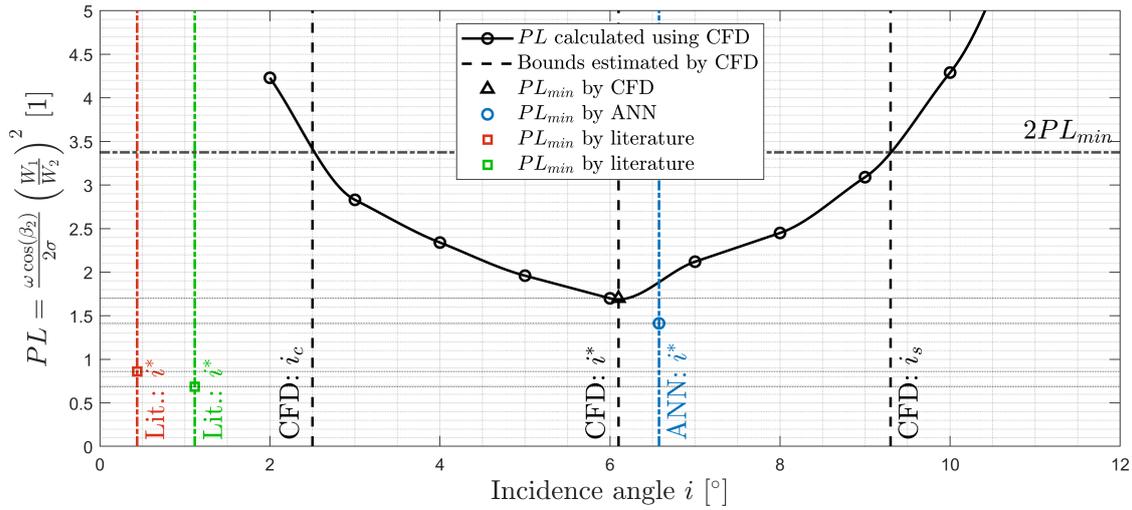
Fig. 10. Design incidence angle i^* and total pressure loss PR predictions comparison for the profile excluded from the training data set

the initial estimate of α^* by the literature correlation does not lead to a more accurate prediction of the remaining parameters.

The comparison of the design incidence angle estimation and the total pressure loss is in Fig. 10. The angles i_c, i_s denote positive and negative stall incidence angles, which bound the range of acceptable incidence angles until total pressure loss increases twice [7, 12]. It can be seen that although the estimation difference in the other parameters (in Fig. 9) is not significant, the incidence angle predicted by the correlations from the literature exceeds this range, thus, it is unsuitable for the studied family of airfoils.

Deviations from the ANN approach and from the correlations from the literature compared to the data obtained by CFD are listed in Table 5, both measured with relative error related to the value from CFD as

$$\text{Error} = \frac{\phi - \phi_{CFD}}{\phi_{CFD}}. \tag{21}$$

The only worse predicted flow parameter is the angle of attack α^* in the presented case. The worst predicted parameter from the literature correlations is the design incidence angle i^*, where the error reached up to 92.8 % and 81.7 % in the case of the original and optimized correlations, respectively. The lower error in the predicted i^*, when optimized correlation is used,

Table 5. Mean square error comparison

Parameter	α^*	i^*	δ^*	W_2/W_1	D_{eq}	PL
CFD	17.32	6.10	8.00	0.61	2.11	1.21
Lit.	14.09	0.44	6.61	0.79	1.61	0.86
Opt. Lit.	12.34	1.12	10.96	0.81	1.56	0.69
ANN	11.55	6.57	7.17	0.72	1.80	1.47
Lit. : Error	−18.6 %	−92.8 %	−17.3 %	30.3 %	−23.9 %	−28.8 %
Opt. Lit. : Error	−28.8 %	−81.7 %	36.9 %	32.4 %	−26.3 %	−43.2 %
ANN : Error	−33.3 %	7.8 %	−10.4 %	18.1 %	−14.9 %	21.4 %

is balanced by a higher error in the predicted deviation angle δ^* that resulted in worse prediction of the remaining flow parameters, especially that of the pressure loss PL. The prediction performed by ANN for the rest of parameters (except for α^*, i^*) was better by 8 % in average in comparison with the more precise original correlations from the literature. Thus, it can be seen that the approach using artificial neural networks outperformed the available correlations from the literature even in the case of an airfoil, which was excluded from the training data set. This test proved the ANN ability to be a useful tool during the initial stages of axial compressor design.

5. Conclusion

An approach for loss correlation modelling was presented in this paper. Basic terminology of compressor cascades and empirical correlations were introduced. Basic ideas of neural networks and supervised learning approach were discussed. Output of CFD simulations was taken as the input data set and artificial neural networks were taught to predict the angle of attack α^*, the incidence angle i^*, the deviation angle δ^* and the total pressure loss at design point of an axial compressor cascade designed with a new family of airfoils.

The results of the learning were compared against classical empirical models from the literature and against generalized correlations with optimized coefficients for another family of airfoils. The optimization process and found constants were also presented. The approximation using ANN outperformed available correlation models from the literature as could be seen in Tables 2, 3 and 4. The most significant improvement is evident in the design incidence and the deviation angles, where the MSE ratio Lit./ANN reached up to 17.026 and 257.779, respectively. The results obtained using fitted empirical correlations were more accurate, but they were not able to outperform the approach using artificial neural network in terms of MSE.

Finally, there was a test of neural networks prediction on a cascade, which was not included in the training data set. The neural network was able to better predict all parameters except the angle of attack α^*. The rest of parameters was predicted with a maximal error of 21.4 % that is by seven percent better than the second more accurate result. The design incidence angle was estimated with the smallest error of 7.8 %, where the classical correlation from the literature failed completely and predicted this parameter with an error higher than 90 %. The optimized correlation performed better, but with the error still higher than 80 %. The ANN ability to be a useful tool during the initial stages of axial compressor design was demonstrated. It was also shown that neither classical nor generalized correlations with fitted coefficients were able to describe the problem more precisely.

Further work should aim to predict performance of axial compressors at off-design points. Firstly, it will require to extend the training data set involving Mach number effects. In this case, it will be possible to estimate acceptable incidence angles range bounds, i.e., positive and negative stall incidence angles. Secondly, it should be possible to estimate off-design flow parameters, e.g., the deviation angle, loss coefficient and overall behaviour of the device. In the off-design cases, even in the case of compressor pumping, it is very tricky to reach a stable CFD simulation due to the transient nature of the phenomenon, thus, flow parameters are very difficult to obtain. Finally, taught neural networks should be deployed as a library for a CFD solver to accelerate simulations.

Acknowledgements

References

[1] Aungier, R.H., Axial-flow compressors: A strategy for aerodynamic design and analysis, ASME Press, 2003. https://doi.org/10.1115/1.801926

[2] Bublík, O., Heidler, V., Pecka, A., Vimmr, J., Neural-network-based fluid-structure interaction applied to vortex-induced vibration, Journal of Computational and Applied Mathematics 428 (2023) rude115 170. https://doi.org/10.1016/j.cam.2023.115170

[3] Farokhi, S., Aircraft propulsion, John Wiley & Sons, 2014.

[4] Gupta, M. M., Bukovsky, I., Homma, N., Solo, A. M. G., Hou, Z.-G., Fundamentals of higher order neural networks for modeling and simulation, In: Artificial higher order neural networks for modeling and simulation, IGI Global, 2013, pp. 103–133. https://doi.org/10.4018/978-1-4666-2175-6.ch006

[5] Gupta, M. M., Jin, L., Homma, N., Static and dynamic neural networks: From fundamentals to advanced theory, John Wiley & Sons, 2004. https://doi.org/10.1002/0471427950

[6] Herrig, L. J., Emery, J. C., Erwin, J. R., Systematic two-dimensional cascade tests of NACA 65-series compressor blades at low speeds, Technical report ID 19930092353, National Advisory Committee for Aeronautics, Langley Field, 1957.

[7] Howell, A. R., Fluid dynamics of axial compressors, Proceedings of the Institution of Mechanical Engineers 153 (1) (1945) 441–452. https://doi.org/10.1243/PIME_PROC_1945_153_049_02

[8] Johnsen, I. A., Bullock, R. O., Aerodynamic design of axial-flow compressors, Volume 36, Scientific and Technical Information Division, NASA, 1965.

[9] Klesa, J., Aerodynamic design of transsonic compressor airfoil family, Proceedings of the 36th conference with international participation Computational Mechanics, Srní, University of West Bohemia, 2021, pp. 115–118.

[10] Kovář, P., Fürst, J., Compressor cascade total pressure loss correlation modelling at design points using artificial neural networks, Proceedings of the 37th conference with international participation Computational Mechanics, Srní, University of West Bohemia, 2022, pp. 50–53.

[11] Lieblein, S., Incidence and deviation-angle correlations for compressor cascades, Journal of Basic Engineering 82 (3) (1960) 575–584. https://doi.org/10.1115/1.3662666

[12] Lieblein, S., Loss and stall analysis of compressor cascades, Journal of Basic Engineering 81 (3) (1959) 387–397. https://doi.org/10.1115/1.4008481

[13] Lieblein, S., Schwenk, F. C., Broderick, R. L., Diffusion factor for estimating losses and limiting blade loadings in axial-flow-compressor blade elements, Technical report NACA RM E53D01, National Advisory Committee For Aeronautics, Cleveland, 1953.

[14] Salunke, N. P., Channiwala, S. A., Design and analysis of a controlled diffusion aerofoil section for an axial compressor stator and effect of incidence angle and Mach No. on performance of CDA, International Journal of Fluid Machinery and Systems 3 (1) (2010) 20–28. https://doi.org/10.5293/IJFMS.2010.3.1.020